European Journal of Medicinal Chemistry 87 (2014) 631–642

Contents lists available at ScienceDirect

European Journal of Medicinal Chemistry

journal homepage: http://www.elsevier.com/locate/ejmech

Original article

Design and synthesis of Lapatinib derivatives containing a branched side chain as HER1/HER2 targeting antitumor drug candidates

Aifeng Lyu [a, b, 1], Lei Fang [a, 1], Shaohua Gou [a, *]

[a] Jiangsu Province Hi-Tech Key Laboratory for Bio-medical Research and School of Chemistry and Chemical Engineering, Southeast University, Nanjing 211189, China
[b] Jiangsu Hansoh Pharmceutical Corporation, Lianyungang 222000, China

ARTICLE INFO

Article history:
Received 1 June 2014
Received in revised form
29 September 2014
Accepted 2 October 2014
Available online 5 October 2014

Keywords:
Lapatinib derivatives
Tyrosine kinase inhibitors
HER1/HER2 targeting
Antitumor

ABSTRACT

A series of Lapatinib derivatives were designed and prepared by changing the straight alkyl side chain of Lapatinib into a branched one. ELISA assay and western blot analysis showed that these derivatives can significantly inhibit HER1/HER2 as well as their downstream signal transduction proteins. In vitro cytotoxicity assay revealed that these compounds had potent cytotoxic effect against the HER1/HER2-overexpressing cancer cells. A representive compound, **2i**, showed potent in vivo antitumor activity comparable to Lapatinib, which was found to block the cell-cycle progression of BT474 cells in the G1 phase causing tumor cell apoptosis in the flow cytometry study. Moreover, the pharmacokinetic investigation on **2i** also indicated it had a good performance on both absorption and elimination profiles.

1. Introduction

Human epidermal growth factor receptor (EGFR) family, also called HER family, is composed of four tyrosine kinase receptors, which are known as erbB-1/HER1, erbB2/HER2, erbB3/HER3 and erbB4/HER4. The family members such as HER1 and HER2 play a key role in catalyzing phosphorylation reactions in signaling cascades that affect every aspect of cell growth, differentiation and metabolism. The deregulation of HER1 and/or HER2 by gene overexpression, frame deletions or activated somatic mutations has been proven prevalent in many types of cancers including non-small cell lung cancer, head and neck, breast, colon and several other cancers with poor clinical outcome [1]. Thus, they have emerged in recent years as key and validated targets of therapies for solid tumors [2,3]. These receptors consist of an extracellular domain, a single hydrophobic transmembrane segment, and an intracellular portion with a juxtamembrane segment, a protein kinase domain, and a carboxyterminaltail. Like all protein-tyrosine kinase receptors, the HER family members function as homo and heterodimers. But HER-3 has a non-functional kinase, whose induced homodimer formation is unable to stimulate protein kinase activity and downstream signaling. In addition, HER2 fails to bind to any growth factor so that physiological HER2 homodimer formation is unlikely. However, unphysiological overexpression of HER2 leads to the formation of a functional homodimer, which is important in the pathogenesis of many breast cancers [4]. It is believed that the growth factor binding to the receptors can induce a large conformational change in the extracellular domain. In the way to find small molecules as HER protein-tyrosine kinase inhibitors, it is necessary to identify and characterize the catalytic kinase domain. However, the results turned out that the family members share a significant sequence homology with many members of other human kinase. This brings out a unique challenge in the development of selective inhibitors. One way to overcome the problem of selectivity in inhibition is to design ligands that specifically interact with pockets within the kinase active site. These key pockets are localized nearby the adenosine triphosphate (ATP) binding site, which is the natural ligand of HER protein-tyrosine kinase domain. There are two different conformations, namely the active and the inactive, of protein kinases at the ATP binding site. It is known that high specificity can be achieved while targeting the inactive conformation, but while targeting the active conformation the treatment of the diseased state arising from activating mutations is favorable, and the second type of inhibitors has no specificity since they generally act as ATP competitors to inhibit several protein kinases [5]. So far, most of the approved HER protein-tyrosine kinase inhibitors, including Gefitinib, Erlotinib, and Lapatinib (**1**, Fig. 1), target the ATP binding site of the kinase.

* Corresponding author.
E-mail address: sgou@seu.edu.cn (S. Gou).
[1] A. Lyu and L. Fang contributed equally to this work.

http://dx.doi.org/10.1016/j.ejmech.2014.10.006
0223-5234/

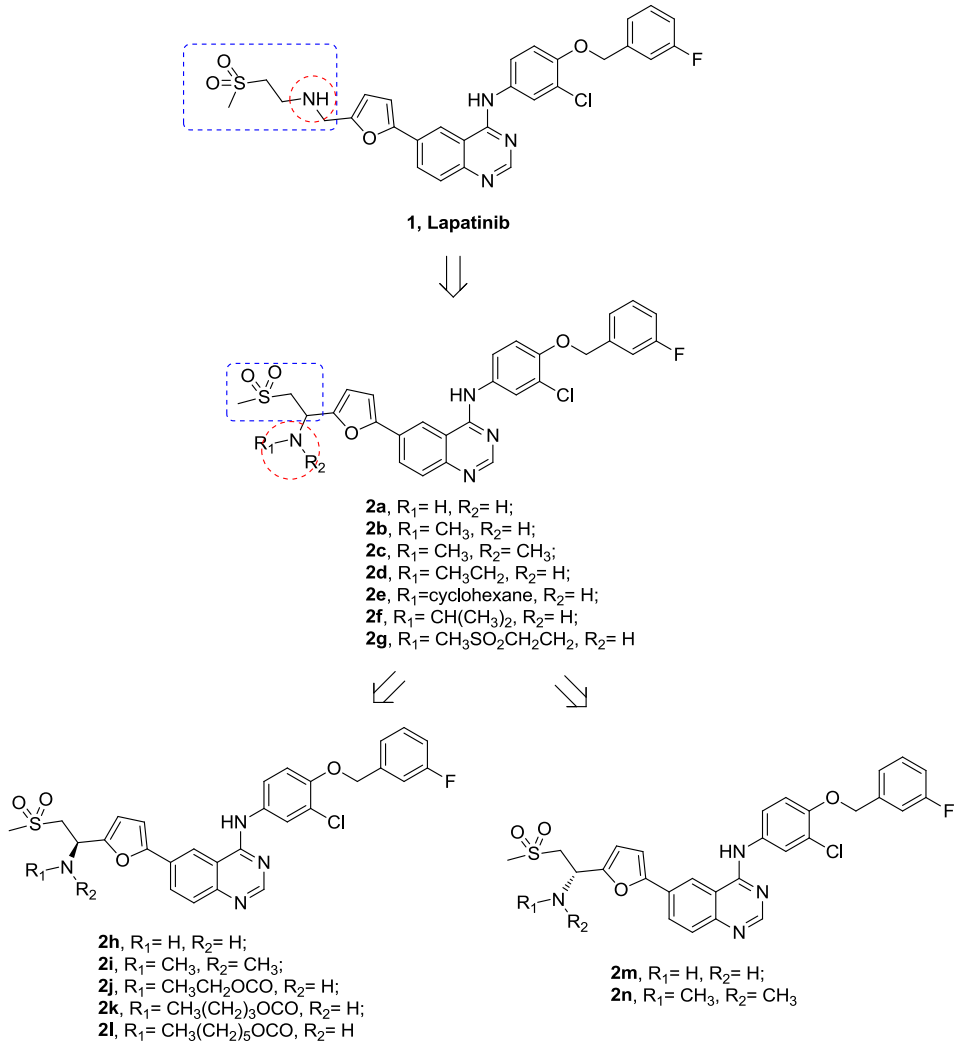

Fig. 1. Structures of Lapatinib and its derivatives **2a**–**n**.

However, Gefitinib and Erlotinib are HER1 inhibitors, whereas Lapatinib is a mixed HER1/HER2 inhibitor. Interestingly, Lapatinib preferentially binds the inactive conformation of HER1 differentiating it from other HER tyrosine kinase inhibitors, such as Erlotinib or Gefitinib. From the structure-interaction point of view, Wood et al. analyzed the complex of HER1 kinase with Lapatinib and found that there are several key interactions with the ATP binding pocket of HER1: the ATP pocket is enlarged in the inactive conformation by rotation and translation of the C-helix, which is necessary to accommodate a 3-fluorobenzyloxy group and explains why Lapatinib can only bind to an inactive conformation; the quinazoline moiety forms the critical H-bond with the hinge region which is similar to those observed for Gefitinib and Erlotinib; the large 3′-chloro-4′-[(3-fluorobenzyl)oxy]aniline group goes into the gatekeeper pocket making mostly hydrophobic contacts [6]. However, the methylsulfonylethylaminomethylfuryl group of Lapatinib, which was found to point into the solvent region, makes no significant contacts with the protein. It is believed that the solvent region generally tolerates a variety of polar functional groups, and the modulation of the side chain in the solvent region may alter the physico-chemical properties of the inhibitors and improve the binding affinity [5,7]. The success of Icotinib that employs a crown ether moiety instead of the two ether chains in Erlotinib is a good example of this strategy [8]. Before long, Dong et al. also reported that four-membered heterocycles-containing Lapatinib analogs showed higher HER protein-tyrosine kinase inhibitory activities and similar antitumor potency, indicating the potency of Lapatinib is still possible to be improved by structural modifications [7]. Based on the above reports, we were encouraged to design and prepare new derivatives by making structural modifications on the side chain. Our strategy is to shorten the length of the side chain of Lapatinib and at the same time change the straight nitrogen-containing chain into a branched one by introducing a substituted amino group, resulting in a series of Lapatinib derivatives containing a branched side chain (Fig. 1). Our preliminary molecular modeling study suggested that the derivative could effectively enter the ATP binding pocket of HER1 and maintain the binding mode of Lapatinib, meanwhile, the side chain moiety extends into the solvent region and makes contacts with residues Asp855 and Thr854 (Fig. 2, A). These preliminarily results supported our rationale that the designed derivatives may retain or even improve the HER1 inhibitory activity of Lapatinib.

2. Results and discussion

2.1. Chemistry

For the synthesis of the derivatives, a similar synthetic procedure previously used for Lapatinib was employed [9]. Generally, the quinazoline compound was coupled to the boronic acid (**4**) via a

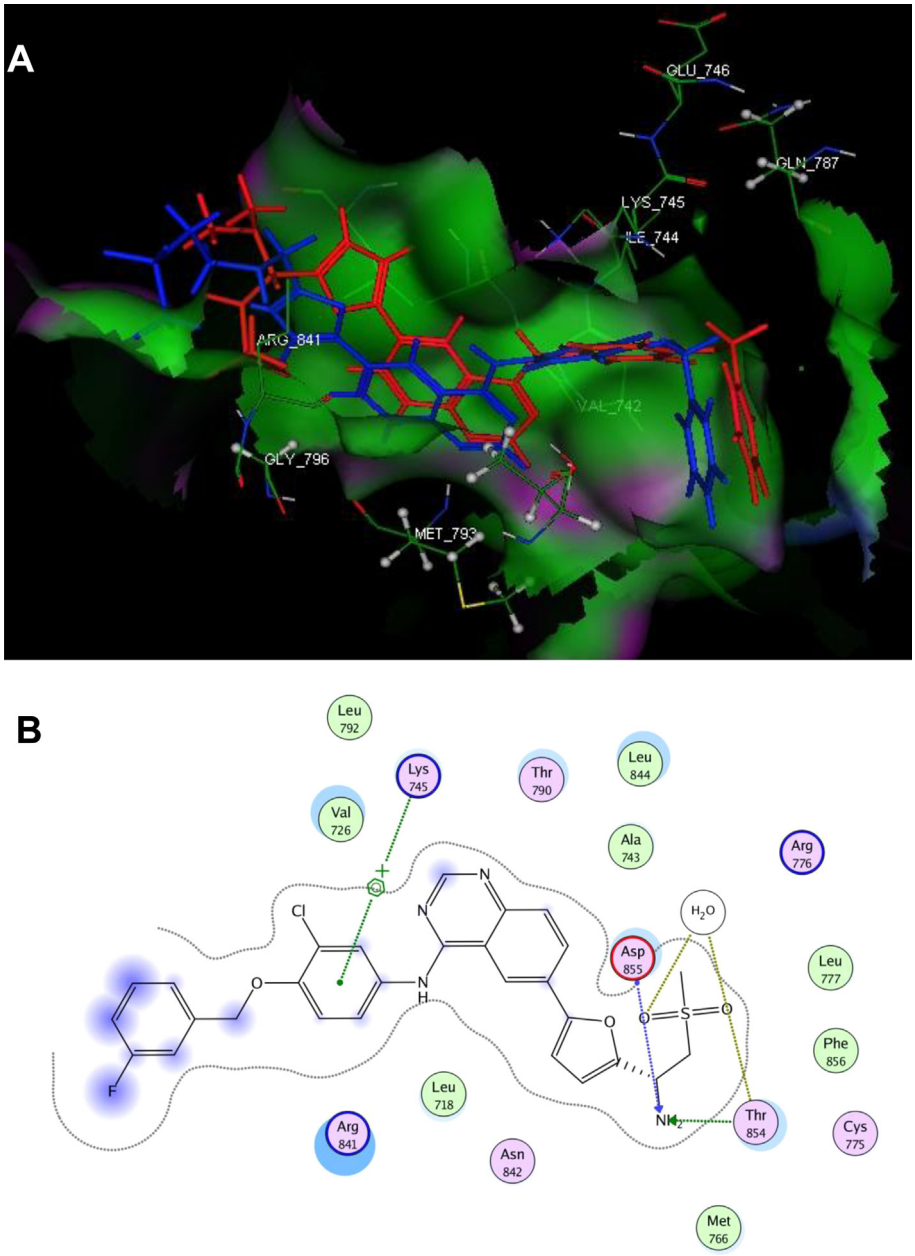

Fig. 2. A) Docking of compound **2i** (shown in red) within the HER1 kinase domain (PDB code: 1XKK) in comparison with Lapatinib (shown in blue). B) The illustration of the interaction mode of **2i** with the corresponding active sites of HER1. Note the new H-bonds formed between Asp855 and Thr854 residues and the amino group of **2i**. (For interpretation of the references to colour in this figure legend, the reader is referred to the web version of this article.)

Suzuki coupling reaction to form the key intermediate **5**. For the synthesis of the racemic products, compound **5** was treated with dimethyl sulfone in the presence of *n*-butyllithium and then refluxed in methanol/40% H_2SO_4 to give compound **6**, which was further reacted with the corresponding alkyl amines to give the final products **2a**–**g**, respectively (Scheme 1). For the synthesis of the stereoisomers **2h**–**n**, the *t*-butanesulfinyl group was used as a powerful chiral directing group [10]. In detail, compound **5** was firstly aminated by (R) or (S)-*t*-butylsulfinamide to give the corresponding (R) or (S)-Schiff's base (**7** or **8**) which was further treated with dimethyl sulfone in the presence of *n*-butyllithium and followed by removing of the sulfinyl group to offer the enantiomers **2h** and **2m**, respectively. Products **2i** and **2n** were obtained by treating **2h** or **2m** with formic acid and 40% formaldehyde aqueous solution in DMSO. For the preparation of the amide products, compound **2h** was directly acylated by the corresponding acyl chloride to offer **2j**–**l**, respectively (Scheme 2).

2.2. Tyrosine kinase inhibition

To examine the potential of the newly synthesized derivatives for use as tyrosine kinase inhibitors, compounds **2a**–**n** were subjected to an ELISA assay [11]. Table 1 shows the inhibitory activity of the derivatives against HER1, HER2, c-Kit, PDGFR and KDR, respectively. It was found that the derivatives significantly inhibited the autophosphorylation of HER1 and HER2 kinases. The IC_{50} values of the derivatives (except the amide products **2j**–**l**) are below 60 nM for HER2 inhibition and within the range of 4.1–22.2 nM for HER1 inhibition. Particularly, compound **2c** showed potent inhibitory activity towards both HER2 and HER1

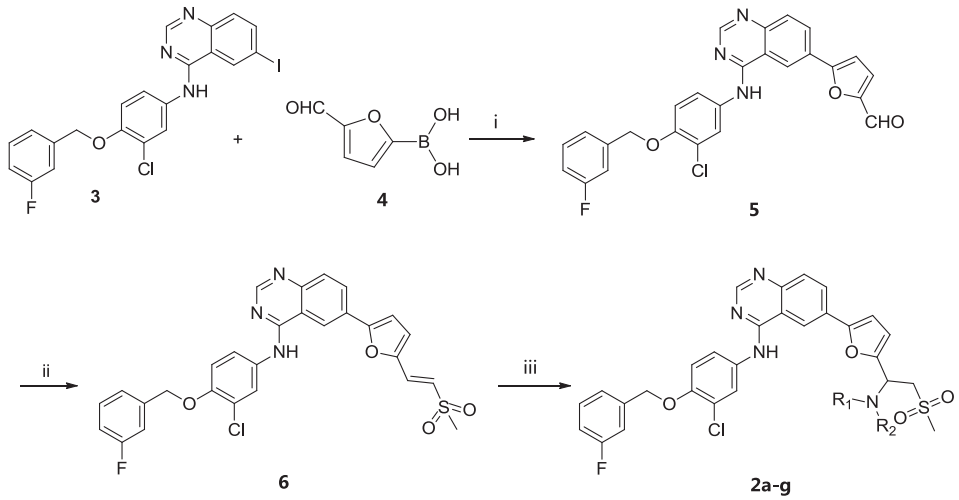

Scheme 1. The synthetic route of compounds **2a**–**g**. Reagents and conditions: i) $(Ph_3P)_2PdCl_2$, NEt_3, MeOH, reflux, 12 h; ii) dimethyl sulfone, *n*-butyllithium, THF, r.t., 4 h; then methanol/40% H_2SO_4, reflux, 4 h; iii) corresponding amine, MeOH, reflux, 24 h.

kinases with IC_{50} values of 3.6 and 6.8 nM, respectively, which is in magnitude at the same order as Lapatinib with IC_{50} value of 2.7 and 7.9 nM, respectively. Considering there is a chiral center at the side chain of **2c**, we managed to prepare two enantiomers **2i** and **2n** via chiral synthesis and investigated whether there is any difference of the activities between the two enantiomers. It turned out that the (S)-isomer **2i** showed higher potency than the (R)-isomer **2n**, indicating that the steric configuration of the side chain has an influence on the activity of the enantiomers. In contrast, compounds **2j**–**l**, which possess amide substituents on the side chain, showed only a weak inhibitory activity with IC_{50} values around 100 nM. All derivatives did not show significant inhibitory effects on c-Kit, PDGFR and KDR kinases, suggesting that the derivatives could be considered as HER1/HER2 selective inhibitors, which are similar to the action manner of the lead compound Lapatinib.

2.3. Western blot analysis

Since compound **2i** showed the best activity in the ELISA assay, it was selected to perform a western blot assay to investigate its effect on the phosphorylation of tyrosine kinases as well as the activation of the downstream signal transduction pathways. It is well known that growth factors (e.g. $VEGF_{165}$, EGF, $PDGF_{BB}$ and SCF-1) binding to the corresponding tyrosine kinase receptors can induce the phosphorylation of the tyrosine kinases, and cause a dose dependent inhibition of biomarker phosphorylation, resulting in a series of biological effects. Though different types of tyrosine kinase receptors share a great degree of commonality, they also have their own specificity [5]. In order to determine the inhibitory effect of **2i** on the different downstream signal transduction pathways, five different cell lines, including NCI-H526 (overexpressing c-Kit), U87MG (overexpressing PDGFR), HUVEC (overexpressing KDR), A431 (overexpressing HER1) and BT474 (overexpressing HER2), were employed in the assay. Consistent with the former tests, **2i** significantly inhibited the phosphorylation of HER1 (in A431) and HER2 (in BT474) as well as the activation of the biomarkers within the downstream signal transduction pathways in a dose dependent manner (Figs. 3 and 4). It is noted that the inhibitory potency of **2i** towards HER2 is even higher than that of Lapatinib. However, both **2i** and Lapatinib had no effect on c-Kit, PDGFR, KDR and their downstream signal transduction proteins (Figs. 5–7).

2.4. In vitro cytotoxicity

Given the positive results of the HER1/HER2 inhibition test, we further investigated the in vitro cytotoxicity of the derivatives against HER2-overexpressing cancer cell lines (e.g. SK-BR-3 and BT474), HER1-overexpressing cancer cell line (e.g. A431), as well as normal cancer cell line MCF-7 without HER1/HER2 expression using Sulforhodamine B (SRB) assay. Lapatinib was used as the positive control. Table 2 revealed that most of the newly synthesized derivatives showed comparable cytotoxicity to Lapatinib against the HER1/HER2 overexpressing cancer cell lines with IC_{50} values below 0.1 μM. Consistent with the order of the HER1/HER2 inhibitory activity, compound **2c** as well as its enantiomers **2i** and **2n** showed higher potency than the other compounds. Particularly, the cytotoxicity of **2i** (IC_{50} 28.8 nM) against BT474 cell line is even over 2-fold higher than that of Lapatinib (IC_{50} 63.9 nM). However, compounds **2j**–**l** that bear amide substituents on the side chain showed only a weak cytotoxic activity. As for the MCF-7 cell line which has no HER1/HER2 expression, the derivatives did not show any cytotoxicity, which is consistent with the performance of Lapatinib as well as with the kinase inhibition results. Upon analyzing the structure–activity relationship, the alkylamine substituents on the side chain seem beneficial for the HER1/HER2 inhibitory and cytotoxic activity; however, converting the amine groups to the amide groups (e.g. **2j**–**l**) remarkably decreases the activity. The size of the substituents also has an influence on the activity. Bulky groups such as cyclohexylamine (**2e**) and 2-(methylsulfonyl)ethylamine (**2g**) seem to have negative effects on the activity, while small groups such as dimethylamine appear optimal for the activity. The steric configuration of the chiral carbon also plays an important role in the activity. It is noted that the (S)-isomers (e.g. compounds **2h** and **2i**) generally showed higher potency than the (R)-isomers (e.g. compounds **2m** and **2n**). Docking study revealed that the amino group on the side chain of **2i** can interact with the Asp855 and Thr854 residues via H-bonds (Fig. 2, B). In contrast, such interaction was not observed in the case of the (R)-isomer. We assumed that this might be the reason for the activity difference of the isomers. These results have also somehow confirmed that the structure of the side chain can not only influence the physico-chemical properties but also affect the kinases inhibitory activity and consequently the cytotoxic activity.

Considering that compounds **2h** and **2i** showed good activity in the preliminary assays, we further investigated the cytotoxicity of

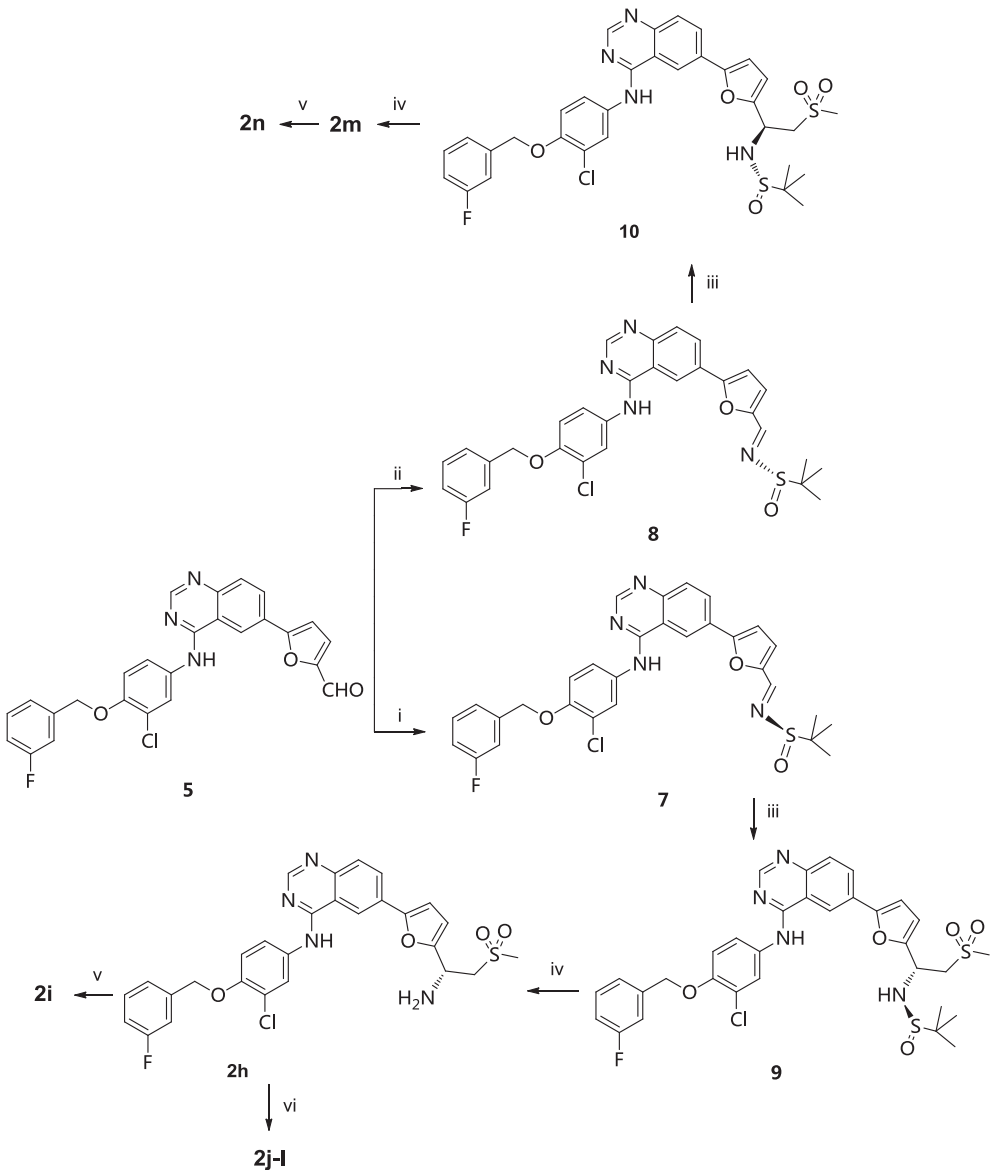

Scheme 2. The synthetic route of compounds **2h**–**n**. Reagents and conditions: i) (R)-*t*-butylsulfinamide, titanium(IV) isopropoxide, THF, reflux, 4 h; ii) (S)-*t*-butylsulfinamide, titanium(IV) isopropoxide, THF, reflux, 4 h; iii) dimethyl sulfone, *n*-butyllithium, THF, −40 °C, 1 h; iv) HCl/ethanol (1:10, v/v), r.t., 30 min; v) HCOOH, 40% HCHO, DMSO, 50 °C, 12 h; vi) corresponding acyl chloride, NEt_3, THF, r.t., 2 h.

Table 1
The tyrosine kinase inhibitory activity of the derivatives **2a**–**n** expressed as IC_{50} values (nM).

Compounds	IC_{50} (nM)[a]				
	HER2	HER1	PDGFRβ	KDR	c-Kit
2a	3.4	17.6	>200,000	>200,000	>200,000
2b	1.0	34.8	>200,000	>200,000	>200,000
2c	3.6	6.8	>200,000	>200,000	>200,000
2d	15.5	14.7	>200,000	>200,000	>200,000
2e	58.6	77.2	>200,000	>200,000	>200,000
2f	48.3	39.2	>200,000	>200,000	>200,000
2g	52.2	28.7	>200,000	>200,000	>200,000
2h	2.9	10.8	>200,000	>200,000	>200,000
2i	0.5	4.1	>200,000	>200,000	>200,000
2j	152.0	89.6	>200,000	>200,000	>200,000
2k	163.8	92.8	>200,000	>200,000	>200,000
2l	158.2	110.2	>200,000	>200,000	>200,000
2m	10.6	13.5	>200,000	>200,000	>200,000
2n	26.1	30.4	>200,000	>200,000	>200,000
Lapatinib	2.7	7.9	>200,000	>200,000	>200,000

[a] Data are the mean values of at least three determinations.

these two compounds against other six cell lines, including HER2 overexpressing Calu-3, MDA-MB-453, SK-OV-3 cancer cell lines, and MDA-MB-231, NCI-H460 cancer cell lines without HER1/HER2 expression as well as normal human lung cell MRC-5 (Table 3). Similar to the former results, both **2h** and **2i** exhibited quite high activity towards the HER1/HER2 expressing tumor cells, while only low or none toxicity to the cells without the expression of HER1/HER2 was observed, indicating a selective cytotoxicity. This result also indicated that HER1 and HER2 are the main action targets of the Lapatinib derivatives.

2.5. Flow cytometry study

Furthermore, a flow cytometry study was performed with **2i** to examine the effect on BT474 cell-cycle progression and the mechanism of cell death (necrosis or apoptosis). The resulting diagrams are shown in Fig. 8. It was observed that, after being co-incubated with BT474 cells for 24 h, both **2i** and Lapatinib could cause accumulation of cells in the G1 phase and produce a decreased

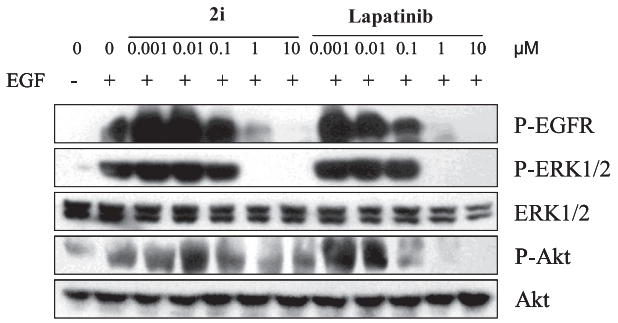

Fig. 3. The effect of **2i** and Lapatinib on HER1 (in A431 cell line) and its downstream signal transduction pathways.

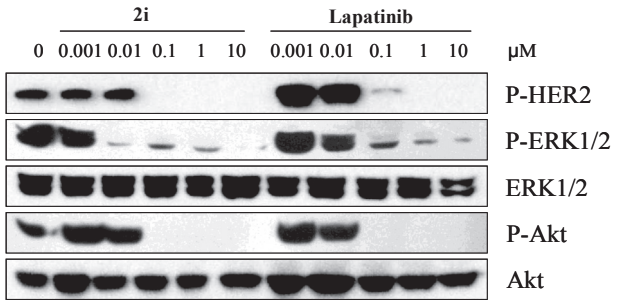

Fig. 4. The effect of **2i** and Lapatinib on HER2 (in BT474 cell line) and its downstream signal transduction pathways.

population of cells in S phase relative to the negative control, indicating that the cell-cycle progression is blocked in the G1 phase by **2i**. In addition, at a dose of 10 μM both **2i** (apoptosis: 11%) and Lapatinib (apoptosis: 13%) showed positive effects on tumor apoptosis.

2.6. In vivo antitumor activity

In view of the good results of the HER1/HER2 inhibition test and the in vitro cytotoxicity assay, compounds **2c** (200 mg/kg, po) and **2i** (100 and 200 mg/kg, po) were selected for further in vivo efficacy studies in a HER2-overexpressing Calu-3 tumor xenograft mouse model (Fig. 9). Lapatinib (100 and 200 mg/kg, po) was used as the positive control and the vehicle (0.5% CMC aqueous solution containing 0.1% Tween-80) group was used as the negative control. It was found that **2i** exhibited significant in vivo efficacy. At a high dose of 200 mg/kg, the tumor inhibiting rate of **2i** reached 83%, much higher than that of Lapatinib (70%), while the tumor inhibiting rate of **2c** (58%) is lower than that of Lapatinib. At a low dose of 100 mg/kg, **2i** still exhibited a good tumor inhibiting activity with an inhibiting rate 68%, superior to the activity of Lapatinib (56%) at the same dose. Furthermore, no body weight loss was observed after the administration of the tested compounds (data not shown),

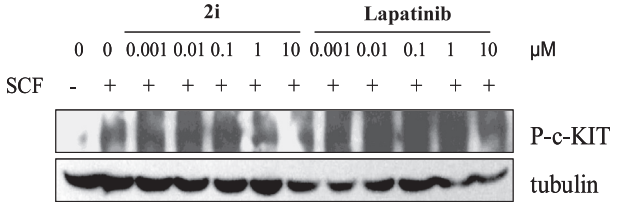

Fig. 5. The effect of **2i** and Lapatinib on c-Kit (in NCI-H526 cell line).

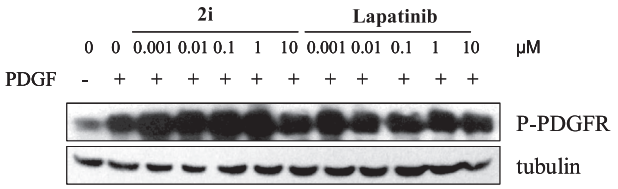

Fig. 6. The effect of **2i** and Lapatinib on PDGFR (in U87MG cell line).

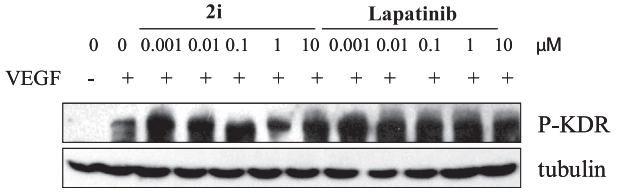

Fig. 7. The effect of **2i** and Lapatinib on KDR (in HUVEC cell line).

Table 2
In vitro cytotoxicity of **2a**–**n** and Lapatinib.

Compd.	IC_{50} (nM)[a]			
	SK-BR-3	BT474	A431	MCF-7
2a	26.6	75.4	682.6	6621
2b	30.1	76.8	648.0	6521
2c	36.2	48.6	604.4	6121
2d	33.9	108.7	884.1	8731
2e	162.2	174.0	773.2	9129
2f	101.2	94.4	623.2	6112
2g	122.8	104.2	683.9	7012
2h	21.0	69.2	662.9	6832
2i	18.4	28.8	634.1	5669
2j	106.0	119.7	884.0	8934
2k	701.5	1005.0	1089.0	9210
2l	1054.0	1919.0	1201.0	>10,000
2m	84.1	116.5	632.2	9336
2n	27.8	83.2	767.7	6666
Lapatinib	30.1	63.9	643.1	8468

[a] Data are the mean values of at least three determinations (IC_{50} is the drug concentration effective in inhibiting 50% of the cell growth measured by SRB assays after 72 h drug exposure).

indicating that the compounds possess a good safety. Thus, on the basis of its potent in vivo efficacy and good in vitro profiles, **2i** was selected as a candidate for further pharmacokinetic investigation.

2.7. Pharmacokinetic investigation

It is well known that the structural modification of the side chain could change the pharmacokinetic properties. For example, the propylmorpholino side chain of the Gefitinib helps to achieve

Table 3
In vitro cytotoxicity of **2h**, **2i** and Lapatinib against HER2 overexpressing Calu-3, MDA-MB-453, SK-OV-3 cancer cell line, and MDA-MB-231, NCI-H460 cancer cell line without HER1/HER2 expression and normal human lung cell MRC-5.

Compd.	IC_{50} (μM)[a]					
	Calu-3	MDA-MB-453	SK-OV-3	MDA-MB-231	NCI-H460	MRC-5
2h	0.22	0.24	0.41	>100	>100	>100
2i	0.23	0.26	0.44	95.31	>100	>100
Lapatinib	0.23	0.19	0.59	>100	>100	>100

[a] Data are the mean values of at least three determinations (IC_{50} is the drug concentration effective in inhibiting 50% of the cell growth measured by SRB assays after 72 h drug exposure).

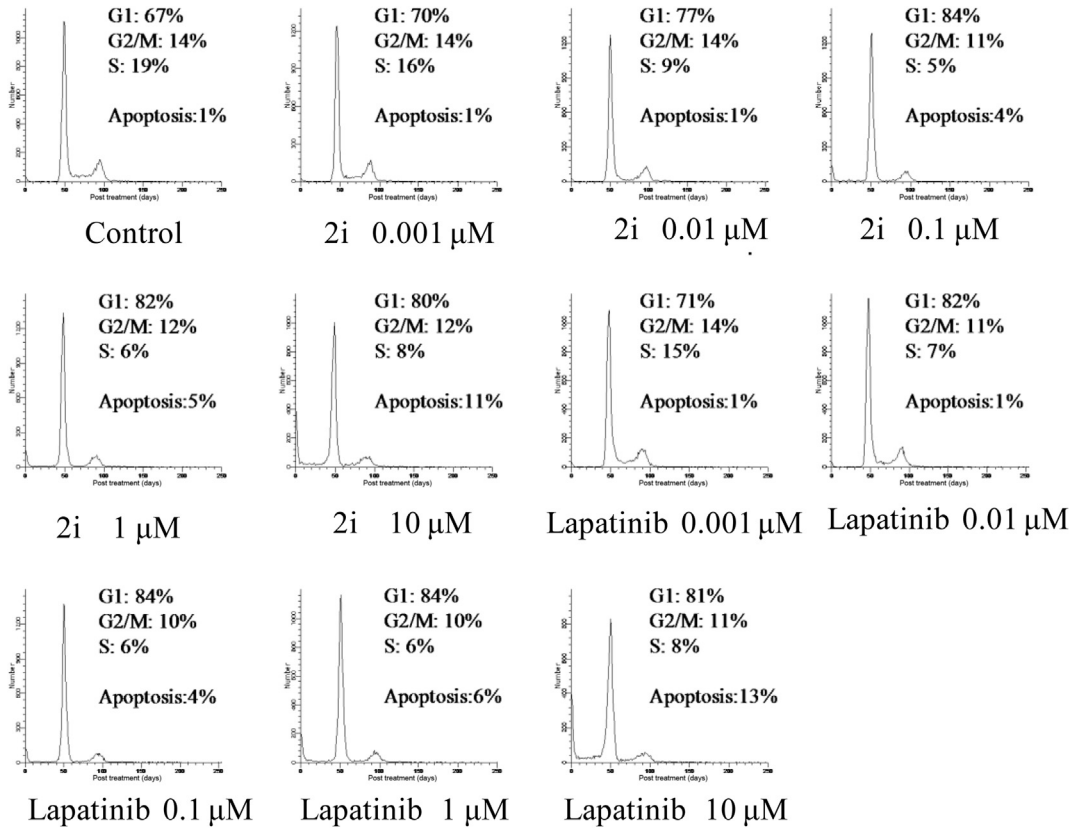

Fig. 8. The effect of **2i** and Lapatinib on BT474 cell-cycle distribution tested by flow cytometry.

high and sustained blood levels in vivo over a 24-h period [5]. In order to investigate whether the branched side chain of the newly synthesized derivatives has an effect on the pharmacokinetic properties or not, compounds **2h** and **2i** were selected for single dose study on the pharmacokinetics property. Beagle dogs were treated with **2h** or **2i** at a dose of 240 mg/kg by gavage, and after 24 h the pharmacokinetic parameters of maximum plasma concentration (C_{max}), time to reach C_{max} (T_{max}), mean residence time (MRT) and area under the plasma concentration–time curve for 0–24 h after dosing ($AUC_{0-24\ h}$) were determined (Table 4). It was noticed that both **2h** and **2i** exhibited good performance in the terms of absorption. The C_{max} and AUC_{0-24h} of **2i** were 3.1 μg/ml and 29.8 μg h/ml, respectively, which is comparable to Lapatinib [12]. Considering single dose study may not accurately predict systemic exposure (AUC) or the half life $t_{1/2}$ since concentrations accumulate with multiple doses [13], multiple dose study was further performed for **2i** (Table 5). After administration of doses of 240 mg/kg for 14 days in 6 beagle dogs, oral absorption was delayed by ~30 min as indicated by T_{max} prolonged from 4.0 h to 4.5 h. The C_{max}, AUC_{0-24h} and $AUC_{0-\infty}$ (area under the plasma concentration–time curve from time zero to infinity after dosing) of **2i** reached 2.9 μg/ml, 30.1 μg h/ml and 30.6 μg h/ml, respectively. As for the elimination profile of **2i**, the elimination half life $t_{1/2}$, the total body clearance *CL* and MRT of **2i** were also determined. The results are shown in Table 4. Judging from both the absorption and elimination profiles of **2i**, it can be concluded that after oral administration **2i** could be effectively absorbed, achieve the therapeutic concentration and maintain the concentration for a long while in vivo. This good pharmacokinetic property may support the potent in vivo efficacy of **2i**.

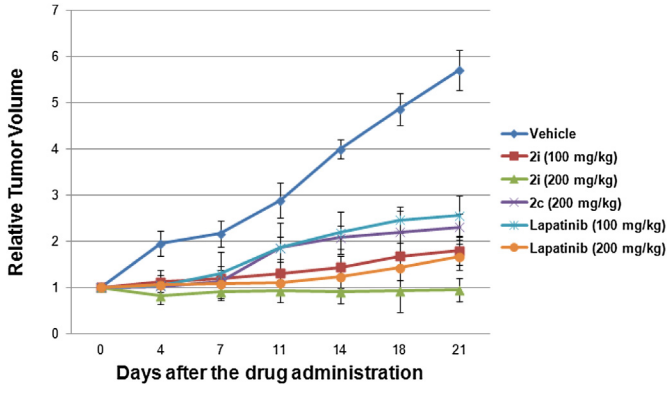

Fig. 9. In vivo anti-tumor effect of different dose of **2c**, **2i** and Lapatinib in Calu-3 tumor-bearing mice models ($n = 6$).

3. Conclusion

HER protein-tyrosine kinases have emerged in recent years as key and validated targets of targeted therapies for solid tumors, thus HER protein-tyrosine kinases inhibitors thereby have attracted

Table 4
Pharmacokinetic parameters of **2h** and **2i** after single dose administration in beagle dogs subjects ($n = 6$).

Compd.	Pharmacokinetic parameters			
	C_{max} (CV%[a]) (μg/ml)	T_{max} (h)	$AUC_{0-24\ h}$ (CV%[a]) (μg·h/ml)	MRT (CV%[a]) (h)
2h	2.1 (37%)	5.0	20.3 (31%)	6.8 (28%)
2i	3.1 (45%)	4.0	29.8 (42%)	6.1 (38%)

[a] CV% means coefficient of variation.

Table 5
Pharmacokinetic parameters of **2i** after multiple dose administration in beagle dogs subjects ($n = 6$).

Compd.	Pharmacokinetic parameters						
	C_{max} (CV%[a]) (μg/ml)	T_{max} (h)	$AUC_{0-24\ h}$ (CV%[a]) (μg·h/ml)	$AUC_{0-\infty}$ (CV%[a]) (μg·h/ml)	*CL* (L/h)	$t_{1/2}$ (h)	MRT (CV%[a]) (h)
2i	2.9 (47%)	4.5	29.8 (29%)	30.6 (36%)	25.9	4.8	6.6 (36%)

[a] CV% means coefficient of variation.

much attention in the field of searching for novel antitumor drug candidates. Our current work is focused on the structural modification of the side chain of HER1/HER2 inhibitor Lapatinib by changing the straight nitrogen-containing alkyl chain into a branched one. It was found that most of the newly synthesized derivatives retained or even improved the inhibitory activity of Lapatinib against HER1/HER2 as well as the downstream signal transduction proteins. In vitro cytotoxicity assay revealed that the target compounds could significantly inhibit the proliferation of the HER1/HER2-overexpressing cancer cells. Particularly, the in vitro cytotoxicity and the kinases inhibition potency of compound **2i** is even 2–5 folds higher than that of Lapatinib. SAR analysis revealed that the alkylamine substituents on the side chain seem beneficial for the HER1/HER2 inhibitory and cytotoxic activity. However, converting the amine groups to the amide groups significantly decreased the activity. Besides, bulky groups on the side chain have negative effects on the activity, while small groups such as dimethylamine group appear optimal for the activity. The steric configuration of the chiral carbon also plays an important role in the activity. It is noted that the (S)-isomers generally showed higher potency than the (R)-isomers.

For the further pharmacological evaluations, the most active compound **2i** was selected for flow cytometry study. It was found that **2i** could block the cell-cycle progression of BT474 cells in the G1 phase and cause tumor cells apoptosis. In vivo assay also showed that **2i** possessed a comparable antitumor activity to Lapatinib. Further pharmacokinetics investigation on **2i** revealed that it had a good performance on both absorption and elimination profiles. Consequently, these derivatives, especially **2i**, are expected to be promising antitumor candidates for further evaluations.

4. Experimental protocols

4.1. Chemistry

4.1.1. Materials and instruments

All chemicals and reagents were of analytical reagent grade and used without further purification. All the solvents were dried by the standard methods wherever needed. Melting points were determined in open capillary tubes on a Meltemp melting point apparatus and uncorrected. ^{1}H NMR and ^{13}C NMR were recorded using a Bruker 400/100 MHz spectrometer and referenced to the residue $CHCl_3$ 7.26 ppm or DMSO-d_6 2.5 ppm. Mass spectra were measured on Finnigan MAT SSQ 710. The purity of the tested compounds was >95% based on the HPLC analysis (Agilent 1200 and the mobile phase was water: acetonitrile = 55:45; the detection wavelength was set at 254 nm). Diastereoselectivity was determined by chiral HPLC analysis (25 cm × 5 μm ID Microsorb Si normal phase column with UV detection at 280 nm and at 254 nm). Retention times (t_R) were given in minutes.

4.1.2. (E)-N-(3-chloro-4-((3-fluorobenzyl)oxy)phenyl)-6-(5-(2-(methylsulfonyl)vinyl)furan-2-yl)quinazolin-4-amine (**6**)

To a solution of methyl sulfone (3.0 g, 32.0 mmol) in 50 ml of THF was added *n*-butyllithium-hexane solution (2.5 M , 11.4 ml). The resulted solution was stirred at room temperature for 1 h, then was added to a solution of compound **5** (3.0 g, 6.0 mmol) [9] dissolved in 250 ml of THF and stirred for another 3 h. Concentrated sulfuric acid (5 ml) was then added and the mixed solution was refluxed for 1 h. Thereafter, the reaction solution was neutralized by saturated $NaHCO_3$ aqueous solution and extracted with CH_2Cl_2 (300 ml × 3). The organic phase was then dried with anhydrous Na_2SO_4, and the solvent was removed under vacuum to give the crude product which was further purified by column chromatography (CH_2Cl_2/MeOH = 60:1) to give the desired product **6** (1.7 g) in 50% yield as a yellow solid. m.p. 94–96 °C. ^{1}H NMR (400 MHz, DMSO-d_6) δ: 10.01 (s, 1H, N*H*), 8.82 (d, J = 4.4 Hz, 1H, Ar*H*), 8.51 (s, 1H, Ar*H*), 8.20 (dd, J = 8.8, 1.6 Hz, 1H, Ar*H*), 8.06 (d, J = 2.0 Hz, 1H, Ar*H*), 7.80 (d, J = 8.4 Hz, 2H, Ar*H*), 7.50–7.44 (m, 1H, Ar*H*), 7.31–7.26 (m, 3H, Ar*H*), 7.20–7.17 (m, 1H, Ar*H*), 7.11–7.09 (m, 1H, Ar*H*), 6.53 (d, J = 3.2 Hz, 1H, Ar*H*), 6.20 (d, J = 14.2 Hz, 1H, Ar*H*), 6.15 (d, J = 14.2 Hz, 1H, Ar*H*), 5.27 (s, 2H, OCH_2), 3.11 (s, 3H, CH_3). ^{13}C NMR (100 MHz, DMSO-d_6)δ: 162.6, 158.1, 157.9, 154.7, 151.9, 150.2, 149.4, 140.1, 133.6, 130.9, 129.1, 128.8, 128.6, 128.1, 124.9, 123.7, 123.1, 121.5, 120.5, 117.2, 115.8, 115.1, 114.8, 114.4, 108.5, 108.3, 69.9, 41.6. MS-ESI (m/z): 550.0 $[M+H]^+$.

4.1.3. General procedure for the synthesis of **2a–g**

Compound **6** (1.0 mmol) was added to a solution of the corresponding amine (8.0 mmol) dissolved in absolute ethanol and then refluxed for 14 h. The resulted solution was cooled to the room temperature, and then the solvent was removed under vacuum to give the crude product which was furtehr purified by column chromatography (CH_2Cl_2/MeOH = 50:1) to give **2a–g**, respectively.

*4.1.3.1. 6-(5-(1-Amino-2-(methylsulfonyl)ethyl)furan-2-yl)-N-(3-chloro-4-((3-fluorobenzyl)oxy)phenyl) quinazolin-4-amine (**2a**).* Yield 66%. m.p. 121–123 °C. ^{1}H NMR (400 MHz, DMSO-d_6)δ: 10.03 (s, 1H, N*H*), 8.88 (d, J = 4.4 Hz, 1H, Ar*H*), 8.56 (s, 1H, Ar*H*), 8.20 (dd, J = 8.8, 1.6 Hz, 1H, Ar*H*), 8.07 (d, J = 2.0 Hz, 1H, Ar*H*), 7.80 (d, J = 8.4 Hz, 2H, Ar*H*), 7.51–7.45 (m, 1H, Ar*H*), 7.36–7.28 (m, 3H, Ar*H*), 7.21–7.16 (m, 1H, Ar*H*), 7.11–7.10 (m, 1H, Ar*H*), 6.57 (d, J = 3.2 Hz, 1H, Ar*H*), 5.27 (s, 2H, OCH_2), 4.52–4.49 (m, 1H, C*H*), 3.63–3.61 (m, 2H, CH_2), 3.12 (s, 3H, CH_3), 2.38 (br, 2H, NH_2). ^{13}C NMR (100 MHz, DMSO-d_6) δ: 162.6, 158.1, 157.9, 154.7, 151.9, 150.2, 149.4, 140.1, 133.6, 130.9, 129.1, 128.8, 128.6, 124.9, 123.7, 123.1, 121.5, 117.2, 115.8, 115.1, 114.8, 114.4, 108.5, 108.3, 69.9, 59.6, 46.2, 43.0. HPLC purity: t_R = 9.00, 99.44%. MS-ESI (m/z): 567.2 $[M+H]^+$.

*4.1.3.2. N-(3-chloro-4-((3-fluorobenzyl)oxy)phenyl)-6-(5-(1-(methylamino)-2-(methylsulfonyl)ethyl)furan-2-yl)quinazolin-4-amine (**2b**).* Yield 69%. m.p. 134–135 °C. ^{1}H NMR (400 MHz, DMSO-d_6) δ: 9.87 (s, 1H, N*H*), 8.75 (d, J = 1.2 Hz, 1H, Ar*H*), 8.57 (s, 1H, Ar*H*), 8.21 (dd, J = 8.8, 2.0 Hz, 1H, Ar*H*), 8.03 (d, J = 2.4 Hz, 1H, Ar*H*), 7.82 (d, J = 8.4 Hz, 1H, Ar*H*), 7.75 (dd, J = 8.8, 2.4 Hz, 1H, Ar*H*), 7.51–7.46 (m, 1H, Ar*H*), 7.36–7.29 (m, 3H, Ar*H*), 7.21–7.17 (m, 1H, Ar*H*), 7.08 (d, J = 3.2 Hz, 1H, Ar*H*), 6.63 (d, J = 3.2 Hz, 1H, Ar*H*), 5.28 (s, 2H, OCH_2), 4.28–4.25 (m, 1H, C*H*), 3.77–3.71 (m, 1H, CH_2-a), 3.60–3.55 (m, 1H, CH_2-b), 3.38 (br, 1H, N*H*), 3.07 (s, 3H, CH_3), 2.29 (s, 3H, CH_3). ^{13}C NMR (100 MHz, DMSO-d_6) δ: 162.7, 158.1, 154.9, 154.7, 152.3, 150.3, 149.4, 140.1, 133.5, 130.9, 129.1, 128.9, 128.6, 124.9, 123.7, 123.1, 121.6, 117.1, 115.7, 115.1, 114.8, 114.4, 110.4, 108.1, 69.9, 57.6, 53.3, 42.7, 33.4. HPLC purity: t_R = 10.10, 96.59%. MS-ESI (m/z): 581.3 $[M+H]^+$.

*4.1.3.3. N-(3-chloro-4-((3-fluorobenzyl)oxy)phenyl)-6-(5-(1-(dimethylamino)-2-(methylsulfonyl)ethyl)furan-2-yl)quinazolin-4-amine (**2c**).* Yield 65%. m.p. 90–92 °C. ^{1}H NMR (DMSO-d_6, 400 MHz) δ: 9.86 (s, 1H, N*H*), 8.73 (d, J = 1.2 Hz, 1H, Ar*H*), 8.57 (s, 1H, Ar*H*), 8.19 (dd, J = 1.6, 8.8 Hz, 1H, Ar*H*), 8.00 (d, J = 2.8 Hz, 1H, Ar*H*), 7.83 (d,

J = 8.8 Hz, 1H, Ar*H*), 7.73 (dd, J = 2.4, 8.8 Hz, 1H, Ar*H*), 7.48–7.46 (m, 1H, Ar*H*), 7.32–7.30 (m, 3H, Ar*H*), 7.19 (td, J = 2.0, 8.8 Hz, 1H, Ar*H*), 7.09 (d, J = 3.6 Hz, 1H, Ar*H*), 6.63 (d, J = 3.2 Hz, 1H, Ar*H*) , 5.28 (s, 2H, OCH_2), 4.34–4.32 (m, 1H, C*H*), 3.94 (dd, J = 8.8, 14.8 Hz, 1H, CH_2-a), 3.72 (dd, J = 5.6, 14.8 Hz, 1H, CH_2-b), 3.04 (s, 3H, CH_3), 2.23 (s, 6H, N(CH_3)$_2$) ; ^{13}C NMR (DMSO-d_6, 100 Hz) δ: 162.6, 158.1, 154.8, 152.4, 151.6, 150.4, 149.4, 140.1, 133.4, 130.9, 129.1, 128.9, 128.6, 125.0, 123.7, 123.2, 121.6, 117.2, 115.7, 115.1, 114.8, 114.4, 111.9, 107.9, 69.9, 57.4, 55.3, 54.6, 42.4, 41.2. HPLC purity: t_R = 17.19, 99.08%. ESI-MS (m/z)595.3 [M+H]$^+$.

*4.1.3.4. N-(3-chloro-4-((3-fluorobenzyl)oxy)phenyl)-6-(5-(1-(ethylamino)-2-(methylsulfonyl)ethyl)furan-2-yl)quinazolin-4-amine (**2d**).* Yield 57%. m.p. 97–99 °C. ^{1}H NMR (400 MHz, DMSO-d_6) δ: 9.86 (s, 1H, N*H*), 8.73 (d, J = 1.6 Hz, 1H, Ar*H*), 8.56 (s, 1H, Ar*H*), 8.20 (dd, J = 8.8, 1.6 Hz, 1H, Ar*H*), 8.02 (d, J = 2.4 Hz, 1H, Ar*H*), 7.82 (d, J = 8.8 Hz, 1H, Ar*H*), 7.74 (dd, J = 8.8, 2.4 Hz, 1H, Ar*H*), 7.51–7.45 (m, 1H, Ar*H*), 7.36–7.29 (m, 3H, Ar*H*), 7.21–7.16 (m, 1H, Ar*H*), 7.06 (d, J = 3.2 Hz, 1H, Ar*H*), 6.61 (d, J = 3.2 Hz, 1H, Ar*H*), 5.28 (s, 2H, OCH_2), 4.35–4.32 (m, 1H, C*H*), 3.74–3.51 (m, 2H, CH_2), 3.31 (br, 1H, N*H*), 3.07 (s, 3H, CH_3), 2.63–2.45 (m, 2H, CH_2), 1.03 (t, J = 7.2 Hz, 3H, CH_3). ^{13}C NMR (100 MHz, DMSO-d_6) δ: 162.6, 158.1, 155.3, 154.7, 152.2, 150.3, 149.4, 140.1, 133.5, 130.9, 129.1, 128.9, 128.6, 124.9, 123.7, 123.1, 121.6, 117.0, 115.7, 115.1, 114.8, 114.4, 110.1, 108.1, 69.9, 58.0, 51.6, 42.9, 40.9, 15.4. HPLC purity: t_R = 13.53, 95.12%. MS-ESI (m/z): 595.3 [M+H]$^+$.

*4.1.3.5. N-(3-chloro-4-((3-fluorobenzyl)oxy)phenyl)-6-(5-(1-(cyclohexylamino)-2-(methylsulfonyl)ethyl)furan-2-yl)quinazolin-4-amine (**2e**).* Yield 73%. m.p. 80–81 °C. ^{1}H NMR (400 MHz, DMSO-d_6) δ: 9.86 (s, 1H, N*H*), 8.75 (d, J = 1.6 Hz, 1H, Ar*H*), 8.56 (s, 1H, Ar*H*), 8.20 (dd, J = 8.8, 1.6 Hz, 1H, Ar*H*), 8.00 (d, J = 2.4 Hz, 1H, Ar*H*), 7.83 (d, J = 8.8 Hz, 1H, Ar*H*), 7.74 (dd, J = 8.8, 2.4 Hz, 1H, Ar*H*), 7.50–7.45 (m, 1H, Ar*H*), 7.34–7.28 (m, 3H, Ar*H*), 7.20–7.17 (m, 1H, Ar*H*), 7.04 (d, J = 3.2 Hz, 1H, Ar*H*), 6.63 (d, J = 3.2 Hz, 1H, Ar*H*), 5.28 (s, 2H, OCH_2), 4.37–4.35 (m, 1H, C*H*), 3.76–3.64 (m, 2H, CH_2), 3.41 (br, 1H, N*H*), 3.07 (s, 3H, CH_3), 2.64–2.55 (m, 1H, C*H*), 1.61–1.17 (m, 10H, (CH_2)$_5$). ^{13}C NMR (100 MHz, DMSO-d_6) δ: 162.5, 158.0, 155.3, 154.9, 152.0, 150.3, 149.2, 140.1, 133.5, 130.9, 129.1, 128.9, 128.2, 124.8, 123.3, 122.7, 121.1, 117.9, 115.8, 115.6, 114.6, 113.5, 110.0, 108.7, 69.6, 59.9, 53.0, 43.2, 42.0, 33.9, 26.8, 25.4. HPLC purity: t_R = 11.26, 96.25%. MS-ESI (m/z): 649.2 [M+H]$^+$.

*4.1.3.6. N-(3-chloro-4-((3-fluorobenzyl)oxy)phenyl)-6-(5-(1-(isopropylamino)-2-(methylsulfonyl)ethyl)furan-2-yl)quinazolin-4-amine (**2f**).* Yield 79%. m.p. 86–88 °C. ^{1}H NMR (400 MHz, DMSO-d_6) δ: 9.86 (s, 1H, N*H*), 8.77 (d, J = 1.6 Hz, 1H, Ar*H*), 8.56 (s, 1H, Ar*H*), 8.22 (dd, J = 8.8, 1.6 Hz, 1H, Ar*H*), 8.01 (d, J = 2.4 Hz, 1H, Ar*H*), 7.83 (d, J = 8.8 Hz, 1H, Ar*H*), 7.72 (dd, J = 8.8, 2.4 Hz, 1H, Ar*H*), 7.51–7.46 (m, 1H, Ar*H*), 7.34–7.28 (m, 3H, Ar*H*), 7.20–7.16 (m, 1H, Ar*H*), 7.02 (d, J = 3.2 Hz, 1H, Ar*H*), 6.62 (d, J = 3.2 Hz, 1H, Ar*H*), 5.28 (s, 2H, OCH_2), 4.37–4.35 (m, 1H, C*H*), 3.76–3.64 (m, 2H, CH_2), 3.35 (br, 1H, N*H*), 3.07 (s, 3H, CH_3), 2.62–2.59 (m, 1H, C*H*), 0.99 (d, 6H, J = 7.2 Hz, (CH_3)$_2$). ^{13}C NMR (100 MHz, DMSO-d_6) δ: 162.4, 158.1, 157.9, 154.7, 151.5, 150.2, 149.2, 140.1, 133.6, 130.2, 129.0, 128.8, 128.6, 124.9, 123.7, 122.9, 121.5, 117.2, 115.8, 115.1, 114.8, 114.4, 108.5, 108.3, 69.9, 59.9, 50.7, 46.2, 43.0, 22.5. HPLC purity: t_R = 9.29, 98.71%. MS-ESI (m/z): 609.1 [M+H]$^+$.

*4.1.3.7. N-(3-chloro-4-((3-fluorobenzyl)oxy)phenyl)-6-(5-(2-(methylsulfonyl)-1-((2-(methylsulfonyl)ethyl) amino)ethyl)furan-2-yl)quinazolin-4-amine (**2g**).* Yield 42%. m.p. 79–80 °C. ^{1}H NMR (400 MHz, DMSO-d_6) δ: 9.87 (s, 1H, N*H*), 8.75 (d, J = 1.6 Hz, 1H, Ar*H*), 8.55 (s, 1H, Ar*H*), 8.22 (dd, J = 8.8, 1.6 Hz, 1H, Ar*H*), 8.01 (d, J = 2.4 Hz, 1H, Ar*H*), 7.83 (d, J = 8.8 Hz, 1H, Ar*H*), 7.72 (dd, J = 8.8, 2.4 Hz, 1H, Ar*H*), 7.55–7.51 (m, 1H, Ar*H*), 7.36–7.29 (m, 3H, Ar*H*), 7.21–7.18 (m, 1H, Ar*H*), 7.02 (d, J = 3.2 Hz, 1H, Ar*H*), 6.62 (d, J = 3.2 Hz, 1H, Ar*H*), 5.28 (s, 2H, OCH_2), 4.39–4.36 (m, 1H, C*H*), 3.79–3.59 (m, 4H, SO_2CH_2, SO_2CH_2CH$_2$), 3.45 (br, 1H, N*H*), 3.07 (s, 3H, CH_3), 3.02 (s, 3H, CH_3), 2.51–2.48 (m, 2H, CH_2), 0.99 (d, 6H, J = 7.2 Hz, (CH_3)$_2$). ^{13}C NMR (100 MHz, DMSO-d_6) δ: 162.7, 157.9, 157.6, 154.0, 152.1, 150.9, 149.1, 140.0, 135.1, 130.9, 129.0, 128.2, 128.0, 124.2, 123.8, 122.9, 121.0, 117.3, 115.3, 115.0, 114.9, 114.2, 109.8, 108.7, 69.9, 60.1, 51.2, 50.3, 43.9, 43.1, 34.5. HPLC purity: t_R = 11.21, 97.01%. MS-ESI (m/z): 673.2 [M+H]$^+$.

*4.1.4. Gerneal procedure for the synthesis of **9** and **10***

A mixture of compound **5** (1.0 mmol), (R) or (S)-*t*-butylsulfinamide (1.2 mmol), titanium(IV) isopropoxide (3 mmol) in THF (15 ml) was refluxed for 4 h. After cooled to the room temperature, the mixture was treated with saturated NaCl aqueous solution and a great amount of deposit was formed. The deposit was filtrated off. The filtrate was then concentrated, diluted by CH_2Cl_2, and washed by water. Then, the organic phase was separated, dried with anhydrous Na_2SO_4, and the solvent was removed under vacuum to give the desired product (**7** or **8**) as yellow oil which was applied in the next reaction without purification.

To a −40 °C solution of methyl sulfone (6.0 mmol) in THF (15 ml) was slowly added a solution of *n*-butyllithium (4.0 mmol) in *n*-hexane, and the resulted solution was stirred at −40 °C for 0.5 h. Compound **7** or **8** obtained from the last step (1.0 mmol) in 15 ml of THF was then quickly added, and the resulted solution was stirred at −40 °C for another 0.5 h. Thereafter, the reaction solution was poured into 200 ml of saturated NaCl aqueous solution. The organic phase was separated, dried with anhydrous Na_2SO_4, and the solvent was removed under vacuum to give the crude product which was further purified by column chromatography (CH_2Cl_2/MeOH = 60:1) to give the desired product (**9** or **10**).

*4.1.4.1. (S)-N-(1-(5-(4-((3-chloro-4-((3-fluorobenzyl)oxy)phenyl) amino)quinazolin-6-yl)furan-2-yl)-2-(methylsulfonyl)ethyl)-2-methylpropane-2-sulfinamide (**9**).* Yield 57%. m.p. 103–105 °C. $[\alpha]_D^{20}$ = 15.4° (c 1, DMSO). e.e. 96% (major enantiomer, t_R = 6.10; minor enantiomer, t_R = 9.03). ^{1}H NMR (400 MHz, DMSO-d_6) δ: 10.01 (s, 1H, N*H*), 8.87 (d, J = 4.4 Hz, 1H, Ar*H*), 8.56 (s, 1H, Ar*H*), 8.21 (dd, J = 8.8, 1.6 Hz, 1H, Ar*H*), 8.07 (d, J = 2.0 Hz, 1H, Ar*H*), 7.80 (d, J = 8.4 Hz, 2H, Ar*H*), 7.52–7.48 (m, 1H, Ar*H*), 7.36–7.29 (m, 3H, Ar*H*), 7.21–7.16 (m, 1H, Ar*H*), 7.11–7.10 (m, 1H, Ar*H*), 6.57 (d, J = 3.2 Hz, 1H, Ar*H*), 5.65 (br, 1 h, N*H*), 5.27 (s, 2H, OCH_2), 4.59–4.55 (m, 1H, C*H*), 3.65–3.61 (m, 2H, CH_2), 3.12 (s, 3H, CH_3), 1.36 (s, 9H, C(CH_3)$_3$). ^{13}C NMR (100 MHz, DMSO-d_6) δ: 162.5, 158.0, 157.9, 154.7, 151.9, 150.6, 149.4, 140.1, 133.2, 130.1, 129.0, 128.3, 128.1, 124.4, 123.5, 123.1, 121.0, 117.7, 115.2, 115.0, 114.1, 113.8, 108.9, 108.6, 69.9, 62.1, 59.9, 46.6, 43.4, 21.5. HPLC purity: t_R = 12.09, 97.14%. MS-ESI (m/z): 671.2 [M+H]$^+$.

*4.1.4.2. (R)-N-(1-(5-(4-((3-chloro-4-((3-fluorobenzyl)oxy)phenyl) amino)quinazolin-6-yl)furan-2-yl)-2-(methylsulfonyl)ethyl)-2-methylpropane-2-sulfinamide (**10**).* Yield 50%. m.p. 103–105 °C. $[\alpha]_D^{20}$ = −16.0° (c 1, DMSO). e.e. 95% (major enantiomer, t_R = 9.03; minor enantiomer, t_R = 6.11).^{1}H NMR (400 MHz, DMSO-d_6) δ: 10.01 (s, 1H, N*H*), 8.87 (d, J = 4.4 Hz, 1H, Ar*H*), 8.56 (s, 1H, Ar*H*), 8.21 (dd, J = 8.8, 1.6 Hz, 1H, Ar*H*), 8.07 (d, J = 2.0 Hz, 1H, Ar*H*), 7.80 (d, J = 8.4 Hz, 2H, Ar*H*), 7.52–7.48 (m, 1H, Ar*H*), 7.36–7.29 (m, 3H, Ar*H*), 7.21–7.16 (m, 1H, Ar*H*), 7.11–7.10 (m, 1H, Ar*H*), 6.57 (d, J = 3.2 Hz, 1H, Ar*H*), 5.65 (br, 1 h, N*H*), 5.27 (s, 2H, OCH_2), 4.59–4.55 (m, 1H, C*H*), 3.65–3.61 (m, 2H, CH_2), 3.12 (s, 3H, CH_3), 1.36 (s, 9H, C(CH_3)$_3$). ^{13}C NMR (100 MHz, DMSO-d_6) δ: 162.5, 158.0, 157.9, 154.7, 151.9, 150.6,

149.4, 140.1, 133.2, 130.1, 129.0, 128.3, 128.1, 124.4, 123.5, 123.1, 121.0, 117.7, 115.2, 115.0, 114.1, 113.8, 108.9, 108.6, 69.9, 62.1, 59.9, 46.6, 43.4, 21.5. HPLC purity: t_R = 12.21, 98.41%. MS-ESI (*m*/*z*): 671.2 $[M+H]^+$.

*4.1.5. General procedure for the synthesis of **2h** and **2m***

Compound **9** or **10** (1.0 mmol) was added into 10 ml of HCl-ethanol solution (1:10, v/v) and the resulted solution was stirred at room temperature for 0.5 h. The reaction solution was then neutralized by 25% aqueous ammonia and extracted by AcOEt (30 ml × 3). The organic phase was dried with anhydrous Na_2SO_4, and the solvent was removed under vacuum to give the crude product which was furtehr purified by column chromatography (CH_2Cl_2/MeOH = 60:1) to give the desired product (**2h** or **2m**).

*4.1.5.1. (S)-6-(5-(1-amino-2-(methylsulfonyl)ethyl)furan-2-yl)-N-(3-chloro-4-((3-fluorobenzyl)oxy)phenyl) quinazolin-4-amine (**2h**).* Yield 64%. m.p. 121–123 °C. $[\alpha]_D^{20}$ = +16.6° (c 1, DMSO). e.e. 94% (major enantiomer, t_R = 7.17; minor enantiomer, t_R = 9.38). ^{1}H NMR (400 MHz, DMSO-d_6)δ: 10.03 (s, 1H, N*H*), 8.88 (d, *J* = 4.4 Hz, 1H, Ar*H*), 8.56 (s, 1H, Ar*H*), 8.20 (dd, *J* = 8.8, 1.6 Hz, 1H, Ar*H*), 8.07 (d, *J* = 2.0 Hz, 1H, Ar*H*), 7.80 (d, *J* = 8.4 Hz, 2H, Ar*H*), 7.51–7.45 (m, 1H, Ar*H*), 7.36–7.28 (m, 3H, Ar*H*), 7.21–7.16 (m, 1H, Ar*H*), 7.11–7.10 (m, 1H, Ar*H*), 6.57 (d, *J* = 3.2 Hz, 1H, Ar*H*), 5.27 (s, 2H, OCH_2), 4.52–4.49 (m, 1H, C*H*), 3.63–3.61 (m, 2H, CH_2), 3.12 (s, 3H, CH_3), 2.38 (br, 2H, NH_2). ^{13}C NMR (100 MHz, DMSO-d_6) δ: 162.6, 158.1, 157.9, 154.7, 151.9, 150.2, 149.4, 140.1, 133.6, 130.9, 129.1, 128.8, 128.6, 124.9, 123.7, 123.1, 121.5, 117.2, 115.8, 115.1, 114.8, 114.4, 108.5, 108.3, 69.9, 59.6, 46.2, 43.0. HPLC purity: t_R = 9.03, 99.13%. MS-ESI (*m*/*z*): 567.2 $[M+H]^+$.

*4.1.5.2. (R)-6-(5-(1-amino-2-(methylsulfonyl)ethyl)furan-2-yl)-N-(3-chloro-4-((3-fluorobenzyl)oxy)phenyl) quinazolin-4-amine (**2m**).* Yield 49%. m.p. 120–123 °C. $[\alpha]_D^{20}$ = −16.2° (c 1, DMSO). e.e. 97% (major enantiomer, t_R = 9.38; minor enantiomer, t_R = 7.17). ^{1}H NMR (400 MHz, DMSO-d_6)δ: 10.03 (s, 1H, N*H*), 8.88 (d, *J* = 4.4 Hz, 1H, Ar*H*), 8.56 (s, 1H, Ar*H*), 8.20 (dd, *J* = 8.8, 1.6 Hz, 1H, Ar*H*), 8.07 (d, *J* = 2.0 Hz, 1H, Ar*H*), 7.80 (d, *J* = 8.4 Hz, 2H, Ar*H*), 7.51–7.45 (m, 1H, Ar*H*), 7.36–7.28 (m, 3H, Ar*H*), 7.21–7.16 (m, 1H, Ar*H*), 7.11–7.10 (m, 1H, Ar*H*), 6.57 (d, *J* = 3.2 Hz, 1H, Ar*H*), 5.27 (s, 2H, OCH_2), 4.52–4.49 (m, 1H, C*H*), 3.63–3.61 (m, 2H, CH_2), 3.12 (s, 3H, CH_3), 2.38 (br, 2H, NH_2). ^{13}C NMR (100 MHz, DMSO-d_6) δ: 162.6, 158.1, 157.9, 154.7, 151.9, 150.2, 149.4, 140.1, 133.6, 130.9, 129.1, 128.8, 128.6, 124.9, 123.7, 123.1, 121.5, 117.2, 115.8, 115.1, 114.8, 114.4, 108.5, 108.3, 69.9, 59.6, 46.2, 43.0. HPLC purity: t_R = 9.12, 99.21%. MS-ESI (*m*/*z*): 567.2 $[M+H]^+$.

*4.1.6. (S)–N-(3-chloro-4-((3-fluorobenzyl)oxy)phenyl)-6-(5-(1-(dimethylamino)-2-(methylsulfonyl)ethyl)furan-2-yl)quinazolin-4-amine (**2i**)*

A mixture of compound **2h** (11.5 g, 20.0 mmol), dimethyl sulfoxide (110 ml), 40% formaldehyde aqueous solution (21 ml), and formic acid (10.6 ml) was stirred at 50 °C for 12 h. Then the solution was diluted by 500 ml of water and the pH value was adjusted to 9 by adding 25% aqueous ammonia dropwise. The formed yellow deposit was collected by filtration and purified by column chromatography (CH_2Cl_2/MeOH = 60:1) to give the desired product **2i** in 78% yield as a yellow solid. m.p. 90–92 °C. $[\alpha]_D^{20}$ = −15.5° (c 1, DMSO). e.e. 98% (major enantiomer, t_R = 7.08; minor enantiomer, t_R = 10.07). ^{1}H NMR (DMSO-d_6, 400 MHz)δ: 9.86 (s, 1H, N*H*), 8.73 (d, *J* = 1.2 Hz, 1H, Ar*H*), 8.57 (s, 1H, Ar*H*), 8.19 (dd, *J* = 1.6, 8.8 Hz, 1H, Ar*H*), 8.00 (d, *J* = 2.8 Hz, 1H, Ar*H*), 7.83 (d, *J* = 8.8 Hz, 1H, Ar*H*), 7.73 (dd, *J* = 2.4, 8.8 Hz, 1H, Ar*H*), 7.48–7.46 (m, 1H, Ar*H*), 7.32–7.30 (m, 3H, Ar*H*), 7.19 (td, *J* = 2.0, 8.8 Hz, 1H, Ar*H*), 7.09 (d, *J* = 3.6 Hz, 1H, Ar*H*), 6.63 (d, *J* = 3.2 Hz, 1H, Ar*H*) , 5.28 (s, 2H, OCH_2), 4.34–4.32 (m, 1H, C*H*), 3.94 (dd, *J* = 8.8, 14.8 Hz, 1H, CH_2-a), 3.72 (dd, *J* = 5.6, 14.8 Hz, 1H, CH_2-b), 3.04 (s, 3H, CH_3), 2.23 (s, 6H, N(CH_3)$_2$). ^{13}C NMR (DMSO-d_6, 100 Hz)δ: 162.6, 158.1, 154.8, 152.4, 151.6, 150.4, 149.4, 140.1, 133.4, 130.9, 129.1, 128.9, 128.6, 125.0, 123.7, 123.2, 121.6, 117.2, 115.7, 115.1, 114.8, 114.4, 111.9, 107.9, 69.9, 57.4, 55.3, 54.6, 42.4, 41.2. HPLC purity: t_R = 17.12, 96.42%. ESI-MS (*m*/*z*)595.3 $[M+H]^+$.

*4.1.7. (R)-N-(3-chloro-4-((3-fluorobenzyl)oxy)phenyl)-6-(5-(1-(dimethylamino)-2-(methylsulfonyl)ethyl)furan-2-yl)quinazolin-4-amine (**2n**)*

Yellow solid, yield 75%. m.p. 90–92 °C. $[\alpha]_D^{20}$ = 15.7° (c 1, DMSO). e.e. 97% (major enantiomer, t_R = 10.07; minor enantiomer, t_R = 7.08). ^{1}H NMR (DMSO-d_6, 400 MHz) δ: 9.86 (s, 1H, N*H*), 8.73 (d, *J* = 1.2 Hz, 1H, Ar*H*), 8.57 (s, 1H, Ar*H*), 8.19 (dd, *J* = 1.6, 8.8 Hz, 1H, Ar*H*), 8.00 (d, *J* = 2.8 Hz, 1H, Ar*H*), 7.83 (d, *J* = 8.8 Hz, 1H, Ar*H*), 7.73 (dd, *J* = 2.4, 8.8 Hz, 1H, Ar*H*), 7.48–7.46 (m, 1H, Ar*H*), 7.32–7.30 (m, 3H, Ar*H*), 7.19 (td, *J* = 2.0, 8.8 Hz, 1H, Ar*H*), 7.09 (d, *J* = 3.6 Hz, 1H, Ar*H*), 6.63 (d, *J* = 3.2 Hz, 1H, Ar*H*), 5.28 (s, 2H, OCH_2), 4.34–4.32 (m, 1H, C*H*), 3.94 (dd, *J* = 8.8, 14.8 Hz, 1H, CH_2-a), 3.72 (dd, *J* = 5.6, 14.8 Hz, 1H, CH_2-b), 3.04 (s, 3H, CH_3), 2.23 (s, 6H, N(CH_3)$_2$). ^{13}C NMR (DMSO-d_6, 100 Hz)δ: 162.6, 158.1, 154.8, 152.4, 151.6, 150.4, 149.4, 140.1, 133.4, 130.9, 129.1, 128.9, 128.6, 125.0, 123.7, 123.2, 121.6, 117.2, 115.7, 115.1, 114.8, 114.4, 111.9, 107.9, 69.9, 57.4, 55.3, 54.6, 42.4, 41.2. HPLC purity: t_R = 17.31, 97.38%. ESI-MS (*m*/*z*)595.3 $[M+H]^+$.

*4.1.8. General procedure for the synthesis of **2j**–**l***

A mixture of 2i (2.0 g, 3.3 mmol), triethylamine (0.4 g, 4.0 mmol) in THF (20 ml) was stirred for 5 min at room temperature. Then corresponding acyl chloride (3.0 mmol) was added and the resulted solution was stirred at room temperature for 2 h. The deposit was filtrated off and the filtrate was concentrated to give the crude product which was further purified by column chromatography (CH_2Cl_2/MeOH = 80:1) to give the desired product **2j**–**l**, respectively.

*4.1.8.1. (S)-ethyl (1-(5-(4-((3-chloro-4-((3-fluorobenzyl)oxy)phenyl)amino)quinazolin-6-yl)furan-2-yl)-2-(methylsulfonyl)ethyl)carbamate (**2j**).* Yellow solid, yield 82%. m.p. 78–80 °C. $[\alpha]_D^{20}$ = 33.2°(c 1, THF). ^{1}H NMR (DMSO-d_6, 400 MHz) δ: 9.88 (s, 1H, N*H*), 8.75 (d, *J* = 1.2 Hz, 1H, Ar*H*), 8.58 (s, 1H, Ar*H*), 8.20 (dd, *J* = 1.6, 8.8 Hz, 1H, Ar*H*), 8.03 (d, *J* = 2.4 Hz, 1H, Ar*H*), 7.99 (br, 1H, N*H*), 7.83 (d, *J* = 8.4 Hz, 1H, Ar*H*), 7.75 (dd, *J* = 2.4, 8.8 Hz, 1H, Ar*H*), 7.51–7.46 (m, 1H, Ar*H*), 7.36–7.29 (m, 3H, Ar*H*), 7.19 (td, *J* = 2.0, 8.8 Hz, 1H, Ar*H*), 7.06 (d, *J* = 3.2 Hz, 1H, Ar*H*), 6.59 (d, *J* = 3.2 Hz, 1H, Ar*H*), 5.35–5.32 (m, 1H, *CH*), 5.28 (s, 2H, OCH_2), 4.07 (q, *J* = 7.2 Hz, 2H, OCH_2CH$_3$), 3.86–3.81 (m, 1H, CH_2-a), 3.73–3.67 (m, 1H, CH_2-b), 3.04 (s, 3H, *CH*$_3$), 1.20 (t, *J* = 7.2 Hz, 3H, OCH$_2$CH_3). ^{13}C NMR (DMSO-d_6, 100 Hz)δ: 163.9, 161.4, 158.1, 156.0, 154.8, 153.8, 152.4, 150.3, 149.5, 140.1, 133.5, 131.0, 129.1, 128.9, 128.4, 124.8, 123.8, 123.0, 121.6, 117.3, 115.7, 115.2, 115.0, 114.8, 114.6, 114.4, 109.9, 108.2, 69.9, 60.7, 56.7, 44.9, 15.0. HPLC purity: t_R = 16.55, 98.37%. MS-ESI (*m*/*z*): 639.1 $[M+H]^+$.

*4.1.8.2. (S)-butyl (1-(5-(4-((3-chloro-4-((3-fluorobenzyl)oxy)phenyl)amino)quinazolin-6-yl)furan-2-yl)-2-(methylsulfonyl)ethyl)carbamate (**2k**).* Yellow solid, yield 85%. m.p. 88–89 °C. $[\alpha]_D^{20}$ = 25.5° (c 1, THF). ^{1}H NMR (DMSO-d_6, 400 MHz) δ: 9.88 (s, 1H, N*H*), 8.76 (d, *J* = 1.2 Hz, 1H, Ar*H*), 8.58 (s, 1H, Ar*H*), 8.20 (dd, *J* = 1.6, 8.8 Hz, 1H, Ar*H*), 8.03 (d, *J* = 2.4 Hz, 1H, Ar*H*), 8.00 (br, 1H, N*H*), 7.83 (d, *J* = 8.4 Hz, 1H, Ar*H*), 7.76 (dd, *J* = 2.4, 8.8 Hz, 1H, Ar*H*), 7.51–7.46 (m, 1H, Ar*H*), 7.36–7.29 (m, 3H, Ar*H*), 7.19 (td, *J* = 2.0, 8.8 Hz, 1H, Ar*H*), 7.06 (d, *J* = 3.2 Hz, 1H, Ar*H*), 6.59 (d, *J* = 3.2 Hz, 1H, Ar*H*), 5.34–5.31 (m, 1H, C*H*), 5.28 (s, 2H, OCH_2), 4.04 (m, 2H, CH_2O), 3.85 (dd, *J* = 4.8, 14.4 Hz, 1H, CH_2-a), 3.72 (dd, *J* = 8.8, 14.4 Hz, 1H, CH_2-b), 3.05 (s, 3H,

CH_3), 1.58–1.55 (m, 2H, CH_2CH_2O), 1.36–1.34 (m, 2H, CH_2CH_3), 0.89 (t, J = 7.2 Hz, 3H, CH_2CH_3). ^{13}C NMR (DMSO-d_6, 100 Hz)δ: 162.6, 158.1, 156.1, 154.8, 153.8, 152.4, 150.3, 149.5, 140.1, 133.5, 130.9, 129.1, 128.9, 128.4, 124.8, 123.7, 123.0, 121.6, 117.3, 115.7, 115.1, 114.8, 114.4, 109.8, 108.22, 69.9, 64.5, 56.7, 45.0, 42.1, 31.1, 19.0, 14.0. HPLC purity: t_R = 23.25, 99.22%. MS-ESI (m/z): 667.4 $[M+H]^+$.

*4.1.8.3. (S)-hexyl (1-(5-(4-((3-chloro-4-((3-fluorobenzyl)oxy)phenyl) amino)quinazolin-6-yl)furan-2-yl)-2-(methylsulfonyl)ethyl)carbamate (**2l**).* Yellow solid, yield 79%. m.p. 101–103 °C. $[\alpha]_D^{20}$ = 22.2° (c 1, THF). ^{1}H NMR (DMSO-d_6, 400 MHz) δ: 9.88 (s, 1H, N*H*), 8.75 (d, J = 1.2 Hz, 1H, Ar*H*), 8.58 (s, 1H, Ar*H*), 8.20 (dd, J = 1.6, 8.8 Hz, 1H, Ar*H*), 8.03 (d, J = 2.4 Hz, 1H, Ar*H*), 8.00 (br, 1H, N*H*), 7.83 (d, J = 8.8 Hz, 1H, Ar*H*), 7.75 (dd, J = 2.4, 8.8 Hz, 1H, Ar*H*), 7.49–7.45 (m, 1H, Ar*H*), 7.36–7.29 (m, 3H, Ar*H*), 7.19 (td, J = 2.0, 8.8 Hz, 1H, Ar*H*), 7.06 (d, J = 3.6 Hz, 1H, Ar*H*), 6.59 (d, J = 3.2 Hz, 1H, Ar*H*), 5.34–5.31 (m, 1H, C*H*), 5.28 (s, 2H, OCH_2), 4.03–4.00 (m, 2H, CH_2O), 3.85–3.80 (m, 1H, CH_2-a), 3.72–3.66 (m, 1H, CH_2-b), 3.04 (s, 3H, CH_3), 1.58–1.22 (m, 8H, $(CH_2)_4$), 1.20 (t, J = 7.2 Hz, 3H, CH_3CH_2). ^{13}C NMR (DMSO-d_6, 100 Hz) δ: 162.7, 158.1, 156.1, 154.8, 153.8, 152.4, 150.3, 149.4, 140.1, 133.5, 131.0, 129.1, 128.9, 128.4, 124.8, 123.7, 123.0, 121.6, 117.3, 115.7, 115.1, 114.8, 114.4, 109.8, 108.2, 69.9, 64.7, 56.7, 45.0, 42.1, 31.3, 29.0, 25.4, 22.4, 14.2. HPLC purity: t_R = 30.70, 97.15%. MS-ESI (m/z): 695.3 $[M+H]^+$.

4.2. Biological studies

4.2.1. Molecular modeling

Homology modeling was carried out using the MOE (Molecular Operating Environment) software (Chemical Computing Group Inc.). Initial minimization was performed within the homology modeling function of MOE. The model from MOE was minimized with a few thousand cycles of minimization using the ABNR (adopted-basis Newton–Raphson) method. Ligands were modeled by positioning them in the active site in accordance with the published crystal structure of the HER1 kinase domain complexed with Lapatinib (PDB code: 1XKK). A 7.5 Å sphere of water molecules was added around the ligand. The entire complex was then subjected to alternate cycles of minimization and dynamics. Each dynamics run was short, about 3 ps. The intent was to get a satisfactory structure for the complex that was consistent with the published crystal structure.

4.2.2. Tyrosine kinase assays

ELISA assay was conducted with the help of the Beckman Coulter (Fullerton, CA) Biomek FX robotic instrument or automated microtiter plate washer for most manipulations. In a typical ELISA assay, 1 μL of 1 mg/ml test compounds or reference standard in DMSO was added to plate wells by the Beckman Coulter Biomek FX robotic instrument. The final DMSO concentration did not exceed 1%, and DMSO controls were employed. Then, 80 μL 5 μM ATP solution diluted in kinase reaction buffer (50 mM HEPES pH 7.4, 20 mM $MgCl_2$, 0.1 mM $MnCl_2$, 0.2 mM Na_3VO_4, 1 mM DTT) was added to each well. Subsequently, the kinase reaction was initiated by the addition of purified tyrosine kinase proteins (20 ng) diluted in 10 μL of kinase reaction buffer solution. After incubation for 1 h at 37 °C, the plate was washed three times with phosphate buffered saline (PBS) containing 0.1% Tween 20 (T-PBS). Next, 100 μL of antiphosphotyrosine (PY99) antibody (1:500 dilution) diluted in T-PBS containing 5 mg/ml BSA was added. After 30 min incubation at 37 °C, the plate was washed three times as before. Horseradish peroxidase-conjugated goat antimouse IgG (100 μL) diluted 1:2000 in T-PBS containing 5 mg/ml BSA was added. The plate was reincubated at 37 °C for 30 min and washed as before. Finally, 100 μL of a solution containing 0.03% H_2O_2 and 2 mg/ml *O*-phenylenediamine in 0.1 M citrate buffer, pH 5.5, was added and samples were incubated at room temperature until color emerged. The reaction was terminated by the addition of 50 μL of 2 M H_2SO_4, and the plate was read using a multiwell spectrophotometer (SPECTRAMAX 190) at 490 nm. The inhibition rate (%) was calculated using the following equation: [1 − (*A*490/*A*490 control)] × 100%. IC_{50} values were obtained by Logit method and were determined from the results of at least three independent tests. The results were analyzed by Graphpad Prism 5.0 software.

4.2.3. Western blot analysis

NCI-H526, U87MG, HUVEC, A431 and BT474 cells were grown to half-confluence in six-well plates, starved in serum-free medium for 24 h, and then exposed to the tested compound at concentration of 0.001, 0.01, 0.1 and 1 μM for 2 h. For analysis of receptor tyrosine kinase phosphorylation and downstream signal transduction pathways, cells were stimulated with 20 ng/ml EGF or SCF-1, or $PDGF_{BB}$ or VEGF (all from R&D Systems, Minneapolis, MN) at 37 °C after the tested compound treatment. Western blot analyses were subsequently performed using a standard procedure [14]. Antibodies against the following were used: phospho-ErbB2 and ErbB2, phospho-ERK1/2 and ERK1/2, phospho-AKT and AKT (all from Cell Signaling Technology, Beverly, MA) and β-tubulin (from Sigma).

4.2.4. Cell proliferation assay

SK-BR-3, BT474, A431, and MCF-7 cell lines were used for the cell proliferation assays. All cell lines were obtained from the American Type Culture Collection. Cells were maintained in RPMI-1640 medium supplemented with 5% fetal bovine serum. Cells were plated in 96-well plates at the densities of 5.0×10^4/ml. On the next day, the tested compounds were dosed at 0.5, 5, 50, 500, 1000, and 5000 ng/ml concentrations and the cells were cultured for 3 days. At the end of incubation, cell survival was determined by the sulforhodamine B assay as previously described. The IC_{50} values were obtained from the growth curves using GraphPad Prism 5.0.

4.2.5. Flow cytometry study

1×10^6 BT474 cells were seeded in a six-well plate and incubated at 37 °C under 5% CO_2 overnight. Then cells were treated with the tested compounds for 12 h. Cells were harvested with trypsin and washed twice with PBS solution. Afterward, cells were fixed in cold 70% ethanol and stored at 4 °C. On the day of analysis, ethanol was removed by centrifugation (5 min, 25 °C, 3000 rpm), and cells were washed twice with PBS, and then treated with RNase (75 kU ml^{-1}) for 30 min at 37 °C. Propidium iodide (PI) was finally added (50 mg/ml), and samples were processed by a flow cytometer (FACScan, Becton Dickson, USA). Cells (1×10^4) were acquired for each sample and recording of PI signal in the FL2 channel. The cell-cycle results were analyzed by FCSExpress software.

4.2.6. In vivo antitumor activity study

Calu-3 tumor cell line was grown in culture, and the cells were washed with PBS, dispersed in a 0.05% (w/v) trypsin solution, and resuspended. After centrifugation for 5 min, the cell pellets were resuspended in PBS and adjusted to a concentration of 1×10^7 cells/ml. BALB/cA nude female mice, 6–7 weeks old, were implanted subcutaneously (s.c.) on the midright side with 2×10^6 Calu-3 tumor cells in 0.2 ml PBS. After the mean Calu-3 tumor volume reached 60–150 mm^3, mice were randomly divided into six groups with six mice per treatment group and twelve mice in the negative control group. Tumors were measured individually with a vernier caliper. Volumes were determined using the formula: tumor volume = length × width^2 × 0.5. Relative tumor volumes (RTV)

were determined using the formula: RTV = V_t/V_0, where V_0 = tumor volume measured at the beginning day of the treatment; V_t = tumor volume measured in the course of the treatment. Therapeutic effects on tumor growth were expressed as mean tumor volumes versus time, calculated as $(1 - T/C) \times 100\%$, where T = treated relative tumor volume and C = control relative tumor volume. At the same time, the weight of each mouse was also measured every other day for 21 d.

4.2.7. Pharmacokinetic study

For the single dose studies, Beagle dogs were administrated with tested compounds at a daily dose of 240 mg/kg by oral gavage. Blood collection was performed at time points of 0.25, 0.5, 1, 1.5, 2, 2.5, 3, 4, 6, 8, 10 and 24 h following administration. Blood samples (~1 ml) from Beagle dogs were collected on ice until centrifugation was performed with in one hour (1000× *g* and 4 °C for 15 min). All plasma samples were stored at −20 °C before analysis. For the multiple dose studies, Beagle dogs were treated with the tested compounds at a daily dose of 240 mg/kg by oral gavage for continuous 14 days. On day 1 and day 14 of administration, blood samples were collected at 0 (predose), 0.25, 0.5, 1, 1.5, 2, 2.5, 3, 4, 6, 8, 10 and 24 h following administration. Plasma concentrations were quantified using a validated LC/MS/MS method [15]. The pharmacokinetic analyses were performed using WinNonlin version 5.2.1 (Pharsight Corporation, Mountain View, CA, USA). The pharmacokinetic parameters included half-life ($t_{1/2}$), area under the plasma concentration versus time curve within the 24-h dosing intervals (AUC_{0-24}) were determined by standard model independent methods based on the plasma concentration-time data. C_{max}, MRT, and T_{max} were determined directly from the plasma concentration-time data.

Acknowledgment

This work is supported by Jiangsu Province Hi-Tech Key Laboratory for Bio-medical Research and Jiangsu Hansoh Pharmceutical Corporation. The authors are thankful to the software support of State Key Laboratory of Natural Medicines, China Pharmaceutical University.

References

[1] J. Mendelsohn, J. Baselga, Semin. Oncol. 33 (2006) 369–385.
[2] P. Traxler, Expert Opin. Ther. Targets 7 (2003) 215–234.
[3] H. Zhong, J.P. Bowen, Curr. Top. Med. Chem. 11 (2011) 1571–1590.
[4] R. Ghosh, A. Narasanna, S.E. Wang, S. Liu, A. Chakrabarty, J.M. Balko, A.M. González-Angulo, G.B. Mills, E. Penuel, J. Winslow, J. Sperinde, R. Dua, S. Pidaparthi, A. Mukherjee, K. Leitzel, W.J. Kostler, A. Lipton, M. Bates, C.L. Arteaga, Cancer Res. 71 (2011) 1871–1882.
[5] L.N. Johnson, Protein kinase inhibitors: contributions from structure to clinical compounds, Q. Rev. Biophys. 42 (2009) 1–40.
[6] E.R. Wood, A.T. Truesdale, O.B. McDonald, D. Yuan, A. Hassell, S.H. Dickerson, B. Ellis, C. Pennisi, E. Horne, K. Lackey, K.J. Alligood, D.W. Rusnak, T.M. Gilmer, L. Shewchuk, Cancer Res. 64 (2004) 6652–6659.
[7] F. Zhao, Z. Lin, F. Wang, W. Zhao, X. Dong, Bioorg. Med. Chem. Lett. 23 (2013) 5385–5388.
[8] S. Hu, G. Xie, D.X. Zhang, C. Davis, W. Long, Y. Hu, F. Wang, X. Kang, F. Tan, L. Ding, Y. Wang, Bioorg. Med. Chem. Lett. 22 (2012) 6301–6305.
[9] R. Jyothi Prasad, B.R. Adibhatla Kali Satya, N. Venkaiah Chowdary, W.O. patent 2010/061,400, June 3, 2010.
[10] J.A. Ellman, Pure Appl. Chem 75 (2003) 39–46.
[11] I. Lazaro, M. Gonzalez, G. Roy, L.M. Villar, P. Gonzalezporque, Anal. Biochem. 192 (1991) 257–261.
[12] P.J. Medina, S. Goodin, Clin. Ther. 30 (2008) 1426–1447.
[13] A.K. Bence, E.B. Anderson, M.A. Halepota, Invest. New. Drugs 23 (2005) 39–49.
[14] X.N. Guo, L. Zhong, J.Z. Tan, J. Li, X.M. Luo, H.L. Jiang, J. Ding, Cancer Biol. Ther. 4 (2005) 1125–1132.
[15] S. Hsieh, T. Tobien, K. Koch, J. Dunn, Rapid Commun. Mass Spectrom. 18 (2004) 285–292.